Global Profile Relaxation and Entropy Dynamics in Turbulent Transport

Kenji IMADERA, Yasuaki KISHIMOTO and Jiquan LI

Department of Fundamental Energy Science, Graduate School of Energy Science, Kyoto University, Gokasho, Uji, Kyoto, 611–0011, Japan

(Received 3 March 2010 / Accepted 9 April 2010)

A hierarchical entropy balance equation retaining the dynamics in the radial direction is introduced to study non-local turbulent transport and the associated global profile relaxation. It consists of first- and second-order equations that describe the entropy dynamics related to thermodynamics/fluid quantity and the corresponding micro-scale phase space fluctuations, respectively. Specifically, the second-order equation describes not only a local entropy production related to heat and density flux (i.e., zonal flow), but also the spatial convection of perturbed entropy. We investigated the entropy dynamics in ion-temperature-gradient driven turbulence based on a global gyrokinetic Vlasov simulation in slab geometry. Entropy convection plays an important role in the relaxation dynamics dominated by the avalanche process. A self-organized relaxed state is established, in which short-wavelength temperature corrugation, i.e., zonal pressure, is regulated by zonal flow shear.

Keywords: phase space entropy, global relaxation, turbulent spreading, gyrokinetic simulation

DOI: 10.1585/pfr.5.019

Turbulent transport in magnetically confined fusion plasmas exhibits various prominent features characterized by different temporal and spatial scales. Zonal modes, such as zonal flow and pressure, which are poloidally and toroidally symmetric macro-scale structures nonlinearly generated from micro-scale turbulence, play an important role in regulating turbulent structure and then transport [1]. These zonal modes are considered to be tightly linked to non-local characteristics of turbulent transport that are not explained by the Gaussian statistics, such as intermittent transport, turbulent spreading [2], and avalanche dynamics, etc. Self-organized critical (SOC) transport [3] is also an example in which the turbulence provides a strong constraint on relaxation, leading to a self-organized stiff temperature profile.

To characterize such transport dynamics, *phase space entropy*, which connects micro-scale turbulent structure to macro-scale thermodynamic quantities, has been introduced [4]. However, the entropy has been generally treated as a global quantity that is integrated over phase space, so that the effects of zonal flow and turbulent spreading do not appear explicitly in the entropy balance equation. As the result, the non-local nature of transport is hardly discussed.

To address this problem, we extend the entropy balance equation by retaining the dynamics in the radial direction. We start with a four-dimensional (4D) gyrokinetic model for electrostatic ion-temperature-gradient (ITG) driven turbulence in slab geometry. The normalized basic equation system is given by the gyrokinetic Vlasov and Poisson equations:

$$\frac{\partial f}{\partial t} - \frac{\partial \Phi}{\partial y}\frac{\partial f}{\partial x} + \frac{\partial \Phi}{\partial x}\frac{\partial f}{\partial y} + v_{\parallel}\frac{\partial f}{\partial z} - \frac{\partial \Phi}{\partial z}\frac{\partial f}{\partial v_{\parallel}} = 0, \tag{1}$$

$$-\nabla_{\perp}^2 \Phi + \tau(\Phi - \langle \Phi \rangle_{yz}) = \int f \mathrm{d}v_{\parallel} - 1, \tag{2}$$

where $f(t; x, y, z, v_{\parallel})$ and $\Phi(t; x, y, z)$ are the gyro-center distribution function for ion and electrostatic potential, respectively, and $\tau \equiv T_{\mathrm{i}}/T_{\mathrm{e}}$. $\langle\ \rangle_{yz}$ denotes the average along the y (poloidal) and z (toroidal) directions. Here, ρ_{i} (ion Larmor radius) $\gg \lambda_{\mathrm{i}}$ (ion Debye length) is assumed.

An entropy balance equation that retains the dynamics in the x (radial) direction is obtained by multiplying Eq. (1) by $1 + \log f$ and integrating it over $(y, z, v_{\parallel})$ space. The equation can be separated by assuming $\varepsilon \sim \delta f / f_0 \sim 1/k_{\perp} L_{\mathrm{T}}$ as an expansion parameter, i.e.,

$$\frac{\partial}{\partial t}\int s^{(1)}\mathrm{d}Z^3 + \frac{1}{2T}\frac{\partial \delta Q_{(0,0)}}{\partial x} - \left\{1 - \frac{1}{2}\log(2\pi T)\right\}\frac{\partial \delta U_{(0,0)}}{\partial x} = 0, \tag{3}$$

$$\frac{\partial}{\partial t}\int s^{(2)}\mathrm{d}Z^3 + \frac{\partial}{\partial x}\int\left(-\frac{\partial \Phi}{\partial y}\right)s^{(2)}\mathrm{d}^3 Z + \frac{\delta U_{(0,0)}}{2L_{\mathrm{T}}} = \frac{\delta Q_{(0,0)}}{2TL_{\mathrm{T}}}, \tag{4}$$

where $\mathrm{d}^3 Z = \mathrm{d}y\mathrm{d}z\mathrm{d}v_{\parallel}$, $L_{\mathrm{T}}(x) = -\partial_x \ln T(x)$ and periodic boundary conditions are employed in the y and z directions. f_0 and $\delta f = f - f_0$ are the Maxwellian distribution function and its perturbed part, respectively. Here,

author's e-mail: imadera@center.iae.kyoto-u.ac.jp

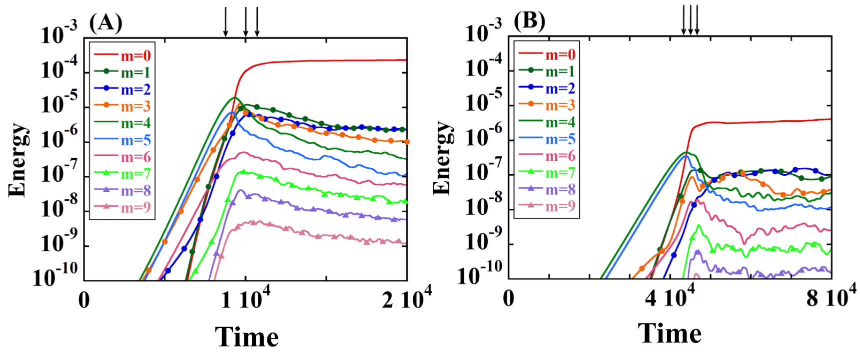

Fig. 1 Time history of the potential energy for each poloidal mode number (m = 0-9) in the case of (A) $L_{\mathrm{T0}} = 37$ and (B) $L_{\mathrm{T0}} = 148$. Arrows mark the time shown in Fig. 2.

the first- and second-order entropies are defined as $s^{(1)} \equiv -\delta f(1 + \log f_0)$ and $s^{(2)} \equiv -\delta f^2/2f_0$. Note that the sum of Eqs. (3) and (4) corresponds to $\mathrm{d}(s^{(1)} + s^{(2)})/\mathrm{d}t = 0$. $\delta U_{(0,0)} \equiv -\int \partial_y \Phi \delta f \mathrm{d}Z^3 = -\int \partial_y \Phi \delta n \mathrm{d}y\mathrm{d}z$ and $\delta Q_{(0,0)} = -\int \partial_y \Phi v_\parallel^2 \delta f \mathrm{d}Z^3 = -\int \partial_y \Phi \delta T \mathrm{d}y\mathrm{d}z$ represent the density and heat flux, respectively. It should be noted that $\delta U_{(0,0)}$ is equivalent to the production rate of zonal flow [5], shown by the relation,

$$\delta U_{(0,0)} = \frac{\partial}{\partial x} \int \frac{\partial \Phi}{\partial y} \frac{\partial \Phi}{\partial x} \mathrm{d}y\mathrm{d}z, \tag{5}$$

which is obtained by multiplying Eq. (2) by $\partial_y \Phi$ and integrating it over (y, z) space, and also from the Hasegawa-Mima equation integrated over (y, z) space,

$$\iint \frac{\partial}{\partial t}\left(\frac{\partial \Phi}{\partial x}\right) \mathrm{d}y\mathrm{d}z - \frac{\partial}{\partial x} \int \frac{\partial \Phi}{\partial y} \frac{\partial \Phi}{\partial x} \mathrm{d}y\mathrm{d}z = 0. \tag{6}$$

The first (EP1), second (HF1) and third (DF1) terms on the left-hand side (LHS) of Eq. (3) correspond to the first-order entropy production related to fluctuation, heat and density flux, respectively, whereas the first (EP2) and third (DF2) terms on the LHS and the first term (HF2) on the right-hand side (RHS) of Eq. (4) represent the corresponding second-order quantities. The second term (EC2) in Eq. (4) represents the divergence of the second-order entropy flux and forms a continuity equation coupled with (EP2). We refer to this process as perturbed entropy convection, which is considered to be related to turbulent spreading. Equation (3) describes the thermodynamics/fluid entropy, which does not produce net entropy. On the other hand, net entropy is produced from (HF2) in Eq. (4), which corresponds to the source term driving the spatial dynamics of $s^{(1)}$ and $s^{(2)}$.

In this study, we investigate the entropy dynamics in ITG turbulence with global profile relaxation using a 4D (i.e., 3D in real space and 1D in velocity space) gyrokinetic full-f Vlasov simulation based on the IDO-CF scheme [6]. We employ a shear-less slab geometry with a system size of $L_x = 2L_y = 64$ and $L_z = 8000$ in real space and $L_v = 10$ in velocity space. Periodic boundary conditions are employed in all the directions (x, y, z) and a grid number of $(N_x, N_y, N_z, N_{v_\parallel}) = (256, 128, 32, 256)$ is typically chosen. The density and electron temperature are assumed to be homogeneous, whereas the ion temperature has a radial profile given by $T(x) = 1 - L_x/(2\pi L_{\mathrm{T0}}) \cos(2\pi x/L_x)$.

Figure 1 illustrates the time history of the potential energy for each poloidal harmonics in two cases: (A) $L_{\mathrm{T0}} = 37$ and (B) $L_{\mathrm{T0}} = 148$. Zonal flows are observed to dominate the saturation and subsequently suppress the turbulence in the both cases, whereas the saturation levels show a difference of about one order in potential amplitude, as expected from the mixing length estimate.

We investigate the entropy balance relation in each term of Eq. (4) given by (EP2), (HF2), (DF2) and (EC2) in Fig. 2 at different times marked by arrows in Fig. 1. The LHS and RHS columns show each term in the case (A) and (B), respectively. The temperature profile is also illustrated.

In Fig. 2 (A1), which shows the phase near saturation, the second-order heat flux (HF2) is induced because of the excitation of ITG mode where the temperature gradient is steep around (a). Note that (HF2) ($\propto \delta Q_{(0,0)}$) is related to the first-order heat flux (HF1) ($\propto \partial_x \delta Q_{(0,0)}$), which causes the temperature relaxation as is found from the relation $\partial_t \delta T_{(0.0)} \cong -\partial_x \delta Q_{(0,0)}$. At this stage, a significant portion of perturbed entropy is found to be convected from the region (a) to both the outer regions (b1) and (b2) (see the profile of (EC2)). Local flattening of the temperature then triggers secondary steepening around (b1) and (b2), so that the subsequent instability takes place. Consequently, as seen in Figs. 2 (A2) and (A3), a step-like temperature profile is exhibited, whereas the front evolves continuously on both sides, accompanied with the coupling between the perturbed entropy production (EP2) and convection (EC2), showing the characteristics of avalanche propagation. Note that the effect of second-order density flux (i.e., zonal flow production) (DF2) is found to be weak in terms of entropy balance in this case.

On the other hand, in the case of (B), where ITG in-

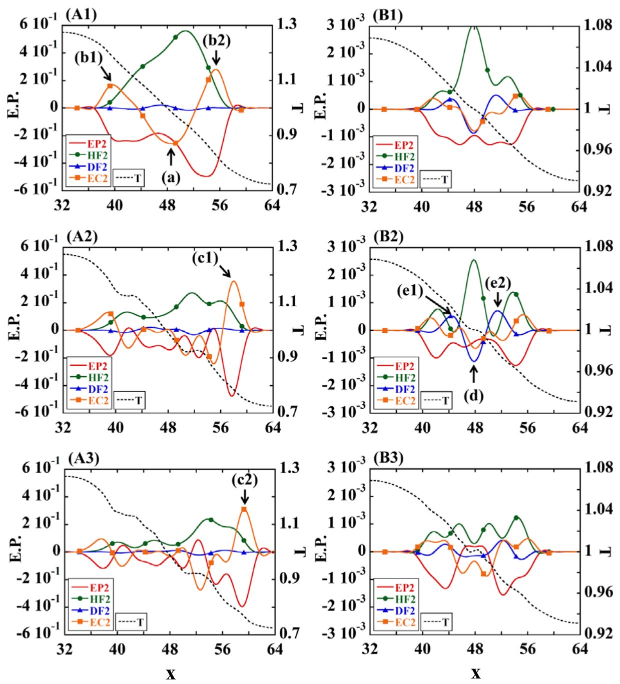

Fig. 2 Spatial profile of each term in the second order entropy balance equation (Eq. (4)) in the case (A) at different times: (A1) 9.0×10^3, (A2) 1.0×10^4, (A3) 1.05×10^4, and in the case (B) at different times: (B1) 4.4×10^4, (B2) 4.5×10^4, (B3) 4.6×10^4. Note that the temperature scale is different.

stability is weak, the effect of perturbed entropy convection (EC2) also becomes weak. Instead, the zonal flow production (DF2) is found to become stronger as seen in Figs. 2 (B1) and (B2). Note that the second-order heat flux (HF2) shows a clear correlation with the zonal flow production (DF2) because (HF2) ($\propto \delta Q_{(0,0)}$) *increases* or *decreases* in the region where (DF2) ($\propto \partial_t(\partial_x \phi_{(0,0)})$) becomes *negative* [(d)] or *positive* [(e1), (e2)], respectively, as seen in Fig. 2 (B2). This result suggests that the observed local temperature relaxation, $\partial_t \delta T_{(0.0)} \cong -\partial_x \delta Q_{(0,0)}$, is related to the production rate of zonal flow shear, i.e., $\partial_t(\partial_x^2 \phi_{(0,0)})$. Namely, the zonal flow locally modulates the heat flux so that a corrugated temperature profile is established. Note that the phase relation between $\delta T_{(0.0)}$ and $\partial_x^2 \phi_{(0,0)}$ (180° out of phase) differs from that of conventional relation of shearing suppression by zonal flows (90° out of phase). A similar phase relation has been discussed in terms of radial force balance in some other studies [7]. Also, spectral analysis shows that $\delta T_{(0.0)}$ has almost same wave number ($k_x^{(z)} \sim 2\pi/6\rho_i$) as $\partial_x^2 \phi_{(0,0)}$. Under these constraints, a self-organized relaxed state with short-wavelength temperature corrugation, i.e., zonal pressure, is globally established, as seen in Fig. 2 (B3). It is considered that the perturbed entropy convection (EC2) plays a role in expanding the radial region of turbulent transport, as in the case of (A).

In conclusion, we investigated the global profile relaxation due to ITG turbulence based on an entropy balance equation retaining the dynamics in the radial direction. We found that the relaxation is dominated by the avalanche-like front propagation in the case of a steep temperature gradient where perturbed entropy convection, which corresponds to turbulent spreading, plays an important role. On the other hand, in the case of a gentle gradient, where the second-order heat flux (HF2) is strongly correlated with the zonal flow production (DF2), a self-organized relaxed state is established, which is characterized by a spatially corrugated short-wavelength zonal pressure. We found that the wave number and phase of the zonal pressure are regulated by the zonal flow shear. Thus, the transport shows qualitatively different characteristics depending on the temperature scale length. The global scale length may be determined by source and sink terms, which needs to be further investigation in future.

This work was supported by the Grant-in-Aid from JSPS (No. 19560828, No. 19560832 and No. 21340171). It was also partially supported by the JSPS-CAS (Japan-China) Core University Program and NIFS/NINS under the projects of Formation of International Network for Scientific Collaborations.

[1] A. Hasegawa and M. Wakatani, Phys. Rev. Lett. **59**, 1581 (1987).
[2] T.S. Hahm, P.H. Diamond, Z. Lin, K. Itoh and S.-I. Itoh, Plasma Phys. Control. Fusion **46**, A323 (2004).
[3] Y. Kishimoto, T. Tajima, W. Horton, M.J. LeBrun and J.Y. Kim, Phys. Plasmas **3**, 1289 (1996).
[4] T.-H. Watanabe and H. Sugama, Phys. Plasmas **9**, 3659 (2002).
[5] P.H. Diamond, O.D. Gurcan, T.S. Hahm, K. Miki, Y. Kosuga and X. Garbet, Plasma Phys. Control. Fusion **50**, 124018 (2008).
[6] K. Imadera, Y. Kishimoto, D. Saito, J.Q. Li and T. Utsumi, J. Comput. Phys. **228**, 8919 (2009).
[7] S.E. Parker, C. Kim and Y. Chen, Phys. Plasmas **6**, 1709 (1999).